Particle Accelerators, 1986, Vol. 20, pp. 23–43
0031-2460/86/2001–0023/$20.00/0

Printed in the United States of America

PRUD-W: A NEW CODE TO COMPUTE AND DESIGN ACCELERATING STRUCTURES

A. G. DAIKOVSKY, YU. I. PARTUGALOV, and A. D. RYABOV
Institute for High Energy Physics, Serpukhov, USSR

(Received July 29, 1985)

We report here a major extension of our earlier work, published in *Particle Accelerators* **12,** 59 (1982). The new code uses a quadrilateral rather than triangular mesh with a higher-order finite-element analysis. Analysis has been extended to periodic structures and includes effects of practical imperfections.

1. INTRODUCTION

The problem of determining eigenfrequencies and eigenelectromagnetic fields in cavities and waveguides has many applications. In particular, it is a major problem in designing accelerating structures and analyzing beam stability in charged-particle accelerators. To solve this problem by numerical methods, there exist only a few computer codes, which can be divided into two categories. Some of these codes have been recently reviewed.[1–3]

The first category includes codes enabling one to compute lower modes in structures having a fairly complicated shape. These codes use the mesh method (finite differences or finite elements) and are designed primarily for frequency tuning of a structure and optimization of the shunt impedance of its operating mode.

The codes of the second category are based on the field-matching method and are used to compute structures of much simpler shapes. But such codes make it possible to compute modes in a very wide frequency range. Such computations are essential for the analysis of beam stability.[3] Papers[3–8] containing references to earlier publications are devoted to specific applications of this method. Though we applied the field-matching method to the problem of optimization of accelerating structures not long ago, its present application can hardly be justified.

The present work has been performed with a view to further developing programs of the first category and enriching them by new facilities. The fact is that tuning and optimization of a cavity does not end with calculating the characteristics of the operating mode. As a rule, the analysis of the whole spectrum of modes in the neighborhood of the operating frequency is required. Since cavities are basically sets of identical (or almost identical) cells, many points concerning their spectral properties are interpreted clearly if one goes over to the study of a waveguide problem, i.e., if the cavity is treated as a section of an

infinite periodic structure. In this case, such notions as the dispersion characteristics of structures and (locally) compensated structures[9] make sense.

Calculation of dispersion characteristics of axially symmetric waves in the Alvarez periodic structure is treated in Ref. 10. It seems somewhat strange that later codes[1,11] (and others; see references in Ref. 1) solve only the cavity-posed problem. This explains why, in order to apply them to the calculation of traveling waves, rather artificial techniques were required.[12]

The present work is devoted to calculating eigenelectromagnetic waves with and without variations in azimuth ($n \geq 0$) in axially symmetric cavities and periodic structures. In the case of periodic structures, any kind of wave ($0 \leq \theta \leq \pi$) can be calculated. According to the Floquet theorem, the problem is posed for one element of periodicity and for an element with a symmetry plane for its half. There is also the possibility of simulating an H-wave structure (RFQ).

The common points taken into account while developing the program are as follows:

(*i*) The choice of variables, the discrete approximation of the boundary problem of electrodynamics, and making the problem an algebraic one.

(*ii*) The method of solution of the algebraic eigenvalue problem.

(*iii*) The calculation of various secondary quantities, e.g., radiotechnical and other characteristics of a structure in normalizations convenient for applications.

(*iv*) The convenient handling of the program, the simple input of the structure data, and the graphic output of data.

It should be noted that items (*i*)–(*ii*) are closely related. Therefore, the application of curvilinear 8-node finite elements,[13] when obtaining discrete approximations of the differential problem, made it possible to reduce considerably the dimensions of mesh spaces as compared to finite-difference approximations and, consequently, to apply the subspace iteration method[14–17] in item (*ii*). When obtaining discrete approximations, another aim was also pursued namely, to conserve the symmetry of electrodynamic equations. This relates to modes with variations in azimuth ($n \geq 1$), i.e., to the fields which cannot be scalarized. Symmetry is conserved providing the equations are written with respect to three field components (**E** or **H**). The symmetry of the matrices makes up for the unavoidable additional calculations in this case.

2. THE PROBLEM FORMULATIONS

To determine the eigen-electromagnetic modes in a volume confined by an ideally conductive metal surface requires one to find the eigenfrequency for which homogeneous Maxwell equations have nontrivial solutions, as well as the solutions themselves. For fields periodically varying in time according to the law $e^{i\omega t}$, the equations have the form

$$\begin{aligned} \nabla \times \mathbf{E} &= -ik\mathbf{H}, & \nabla \cdot \mathbf{E} &= 0, \\ \nabla \times \mathbf{H} &= ik\mathbf{E}, & \nabla \cdot \mathbf{H} &= 0. \end{aligned} \tag{1}$$

The boundary conditions on a metal ($\mathbf{v}$ is a normal) are

$$\mathbf{E} \times \mathbf{v} = 0. \tag{2}$$

Here $\mathbf{E}$ and $\mathbf{H}$ are the complex amplitudes of the field, $k = \omega/c$.

In the case of periodic guide structures, there also exist nontrivial solutions-eigenwaves which may be found in the Floquet representation:

$$\mathbf{E}(x, y, z) = e^{-i\theta z/L}\mathscr{E}(x, y, z),$$
$$\mathbf{H}(x, y, z) = e^{-i\theta z/L}\mathscr{H}(x, y, z),$$

where $\mathscr{E}$ *and* $\mathscr{H}$ *are* L-periodic complex vector functions, L is the geometric period of the structure over z. From these relations there follow equations which are referred to as the quasiperiodicity condition:

$$\begin{aligned} \mathbf{E}(x, y, z + L) &= e^{-i\theta}\mathbf{E}(x, y, z), \\ \mathbf{H}(x, y, z + L) &= e^{-i\theta}\mathbf{H}(x, y, z). \end{aligned} \tag{3}$$

We shall confine ourselves to real values of the parameter θ ($0 \leqslant \theta \leqslant \pi$), which is interpreted as the phase shift per period L; $\mathscr{E}$ and $\mathscr{H}$ determine the wave type and θ its kind. The problems concerning the substantiation of the Floquet representation, as well as the interpretation of the solutions corresponding to the complex values of θ, are briefly treated in Ref. 5, and the original papers are also referenced there.

From Eqs. (1) and (2), it follows that a free electromagnetic field is, generally speaking, characterized by two parameters with the help of which all six field components are expressed. At the same time, in the regions allowing application of the separation of variables method, there exist types of waves with such a polarization that the field is described by just one parameter. These are, in particular, *TM* and *TE* waves in longitudinally homogeneous structures and waves independent of φ in axially symmetric ones. The problems relating to such fields will be called scalar and those relating to the general case will be called vector problems.

For the general case, instead of the problem of Eqs. (1)–(3), we shall consider the problem for a vector wave equation

$$\nabla^2\mathbf{W} + k^2\mathbf{W} = 0, \tag{4}$$

with the boundary conditions on the metal of the first kind,

$$\mathbf{W} \times \mathbf{v} = 0, \qquad \nabla \cdot \mathbf{W} = 0, \tag{5}$$

or the second kind,

$$[\nabla \times \mathbf{W}] \times \mathbf{v} = 0, \qquad \mathbf{W} \cdot \mathbf{v} = 0, \tag{6}$$

where $\mathbf{W}$ means $\mathbf{E}$ and $\mathbf{H}$ in Eqs. (5) and (6), respectively. For the case of a periodic structure, this problem will also have the quasiperiodicity condition

$$\mathbf{W}(x, y, z + L) = e^{-i\theta}\mathbf{W}(x, y, z). \tag{7}$$

The system of eigenfunctions in Eqs. (4)–(7) is known to be the direct sum of

solenoidal and potential subsystems.[18] We shall pay attention to the former, since it is a solution of the initial problem [Eqs. (1)–(3)]. As is easily verified, Eqs. (4)–(7) is a self-conjugated problem producing a functional stationary on eigenfunctions and having on them the corresponding eigenvalues

$$\phi = \frac{\int (|\nabla \times \mathbf{W}|^2 + |\nabla \cdot \mathbf{W}|^2)\, dv}{\int |\mathbf{W}|^2\, dv}. \tag{8}$$

Equation (8) suggests that the spectrum is positive, and since the eigenfunction is either in a solenoidal or potential subsystem, at least for nonmultiple eigenvalues, then

$$k^2 = \frac{\int |\nabla \times \mathbf{W}|^2\, dv}{\int |\mathbf{W}|^2\, dv} \quad \text{or} \quad k^2 = \frac{\int |\nabla \cdot \mathbf{W}|^2\, dv}{|\mathbf{W}|^2\, dv}. \tag{9}$$

These relations will be used to check whether the calculated solution belongs to the solenoidal or potential subsystem. Should the same eigenvalue correspond to both solenoidal and potential eigenfunctions, we are dealing with an invariant subspace produced by them. In this case, one can recommend going over from E components to H components or vice versa. The solenoidal function will correspond to the same field $(\mathbf{E}, \mathbf{H})$, and the spectrum of the potential subsystem will change.

To finish the present section, let us touch upon the questions of symmetry. If a cavity has symmetry planes, then it is sufficient to consider an elementary part of the region and to extend the solution symmetrically or antisymmetrically over these planes into the whole region. The boundary conditions of the first kind correspond to an antisymmetric continuation and those of the second kind to a symmetric one.

If the structure is periodic, we shall draw a distinction between the cases when one can choose the symmetry plane $z = \text{const}$ and when such a plane is absent. Paying attention to Eqs. (4)–(7), we see that $\mathbf{W}$ is determined to an accuracy of an arbitrary phase factor (the modulus $\mathbf{W}$ is determined by the normalisation $\int |\mathbf{W}|^2\, dv = \text{const}$). This arbitrariness may be eliminated in the formulation of the problem for a symmetric period. Indeed, if $-L/2 \leq z \leq L/2$ is the period, with the symmetry plane $z = 0$ and with $\mathbf{W}(x, y, z) = \{W_x(x, y, z), W_y(x, y, z), W_z(x, y, z)\}$ a forward-traveling wave, then $\mathbf{V}(x, y, z) = \{W_x(x, y, -z), W_y(x, y, -z), -(W_z(x, y, -z)\}$ is a backward-traveling wave. But this backward wave is $\mathbf{W}^*(x, y, z)$, which is why $\mathbf{V}(x, y, z)$ and $\mathbf{W}^*(x, y, z)$ differ only by the phase factor $\mathbf{V}(x, y, z) = e^{-i\theta_0}\mathbf{W}^*(x, y, z)$.

Writing down the last relation in component form on the $z = 0$ plane, we obtain

$$e^{i\theta_0} = \frac{W_x}{W_x^*} = \frac{W_y}{W_y^*} = -\frac{W_z}{W_z^*}$$

or

$$e^{i\theta_0} = e^{i2\varphi_x} = e^{i2\varphi_y} = e^{i2(\varphi_z+\pi/2)},$$

where φ_x, φ_y, and φ_z are the phases of the components W_x, W_y, and W_z. Consequently, the wave phase is constant in the plane $z = 0$ and is independent of x and y. Choosing $\theta_0 = 0$ we get

$$\begin{aligned} W_x(x, y, -z) &= W_x^*(x, y, z), \\ W_y(x, y, -z) &= W_y^*(x, y, z), \\ -W_z(z, y, -z) &= W_z^*(x, y, z), \end{aligned} \tag{10}$$

wherefrom there immediately follow the boundary conditions for $\mathbf{W}$ in the plane $z = 0$.

$$\operatorname{Im} W_x = 0, \qquad \operatorname{Im} W_y = 0, \qquad \operatorname{Im} \frac{\partial}{\partial z} W_z = 0,$$

$$\operatorname{Re} \frac{\partial}{\partial z} W_x = 0, \qquad \operatorname{Re} \frac{\partial}{\partial z} W_y = 0, \qquad \operatorname{Re} W_z = 0. \tag{11}$$

Writing down Eq. (10) for $z = L/2$ and applying the quasiperiodicity conditions (Eq. (7)], we get

$$\begin{aligned} e^{i\theta/2} W_x\left(x, y, \frac{L}{2}\right) &= \left[e^{i\theta/2} W_x\left(x, y, \frac{L}{2}\right)\right]^*, \\ l^{i\theta/2} W_y\left(x, y, \frac{L}{2}\right) &= \left[e^{i\theta/2} W_y\left(x, y, \frac{L}{2}\right)\right]^*, \\ -e^{i\theta/2} W_z\left(x, y, \frac{L}{2}\right) &= \left[e^{i\theta/2} W_z\left(x, y, \frac{L}{2}\right)\right]^*. \end{aligned}$$

This yields, in correspondance to Eq. (11), the boundary conditions on the plane $z = L/2$:

$$\begin{gathered} \operatorname{Im} (e^{i\theta/2} W_x) = 0, \qquad \operatorname{Im} (e^{i\theta/2} W_y) = 0, \qquad \operatorname{Im} \left(e^{i\theta/2} \frac{\partial}{\partial z} W_z\right) = 0, \\ \operatorname{Re} \left(e^{i\theta/2} \frac{\partial}{\partial z} W_x\right) = 0, \qquad \operatorname{Re} \left(e^{i\theta/2} \frac{\partial}{\partial z} W_y\right) = 0, \qquad \operatorname{Re} (e^{i\theta/2} W_z) = 0. \end{gathered} \tag{12}$$

The real and imaginary parts of $\mathbf{W}$ are no longer connected for the endpoints of dispersion curves ($\theta = 0$, $\theta = \pi$).

3. SOLUTION OF THE EIGENVALUE PROBLEM

The numerical solution to the problem of Eqs. (4)–(7) will mean its discretization by the finite-element method and its transformation into a problem of algebraic form

$$Aw = \lambda Bw, \tag{13}$$

where, generally speaking, A and B are Hermitian positive-definite matrices, whose complexity is related to the quasiperiodicity condition. It is expedient in Eq. (13) to look not for all the eigenvalues and eigenvectors but only for those pertinent to the low-frequency part of the spectrum. To solve such a partial problem, we apply the inverse iterations method with simultaneous iteration of a few eigenvectors or the shorter subspace iteration method.[14–17]

For real $n \times n$ matrices A and B, this latter method proceeds as follows. Choose m linearly independent vectors and let them form the matrix X_0 of dimension $n \times m$. Then, on the kth step of the iteration process,

(*i*) The system

$$AY_k - \lambda_0 BY_k = BX_{k-1}$$

is solved.

(*ii*) The matrices

$$C_k = Y_k^T AY_k, \qquad D_k = Y_k^T BY_k$$

are formed.

(*iii*) The small eigenvalue problem

$$C_k Q_k = D_k Q_k \Omega_k$$

is solved.

(*iv*) The quantity

$$X_k = Y_k Q_k$$

is calculated.

Step (*i*) singles out a subspace tending, as $k \to \infty$, to an invariant subspace produced by m eigenvectors with the eigenvalue closest to λ_0. Steps (*ii*)–(*iv*) follow from the Rayleigh-Ritz procedure of obtaining the best approximations to these eigenvalues and eigenvectors from the subspace iterated.[17] Step (*i*) is realized in the form of an LU decomposition of the matrix $A - \lambda_0 B$. At step (*iii*) one may use standard routines based on the QR algorithm or the Jacobi method.[16] Note that when finding the eigenvectors of the small problem orthonormalized in D_k norm we obtain automatically the orthonormalized Rayleigh-Ritz approximations and, consequently, eigenvectors in the limit

$$X_k^T BX_k = Q_k^T Y_k^T BY_k Q_k = Q_k^T D_k Q_k = I.$$

In the case of the Hermitian matrices A and B,

$$A = A_1 + iA_2, \quad B = B_1 + iB_2, \quad A_1^T = A_1, \quad A_2^T = -A_2, \quad B_1^T = B_1, \quad B_2^T = -B_2,$$

we shall present them in the form of symmetric extended real matrices

$$A = \begin{vmatrix} A_1 & A_2 \\ A_2^T & A_1 \end{vmatrix}, \qquad B = \begin{vmatrix} B_1 & B_2 \\ B_2^T & B_1 \end{vmatrix}. \tag{14}$$

It is evident that if $w = |u, v|^T$ is an eigenvector then $\bar{w} = |-v, u|^T$ is also an eigenvector orthogonal to w in B norm ($\bar{w}^T Bw = 0$), i.e., each eigenvalue is degenerated at least twice.

The properties of the matrices A and B allow an economic realization of steps (i)–(iv). Let matrix X again be a matrix of linearly independent columns. The dimension of X is $2n \times m$ and that of u, v is n. Let us form the matrix $|X \mid \bar{X}|$, which will be taken as the initial approximation. Then (the index k is left out),

$(i)'$ The system

$$AY - \lambda_0 BY = BX$$

is solved and the system $A\bar{Y} - \lambda_0 B\bar{Y} = B\bar{X}$ is not solved (economy).

$(ii)'$ The matrices $C = |Y \mid \bar{Y}|^T A\,|Y \mid \bar{Y}|$, $D = |Y \mid \bar{Y}|^T B\,|Y \mid \bar{Y}|$ are formed. In this case,

$$C = \begin{vmatrix} C_1 & C_2 \\ C_2^T & C_1 \end{vmatrix}, \qquad D = \begin{vmatrix} D_1 & D_2 \\ D_2^T & D_1 \end{vmatrix},$$

where $C_1 = Y^T AY$, $D_1 = Y^T BY$, $C_2 = Y^T A\bar{Y}$ and, $D_2 = Y^T B\bar{Y}$. The matrices C_1 and D_1 are symmetric, and C_2 and D_2 are antisymmetric (the economy comes from the convolutions when the matrices C and D were formed).

$(iii)'$ The small problem

$$CQ = DQ\Omega$$

is solved. As is easily seen, the matrices C and D inherit the properties of A and B, which is why the small problem takes the form

$$C\,|R \mid \bar{R}| = D\,|R \mid \bar{R}| \begin{vmatrix} Q_m & 0 \\ 0 & Q_m \end{vmatrix},$$

where $Q_m = \operatorname{diag}(\omega_1, \ldots, \omega_m)$ is the matrix of eigenvalues, and $Q = |R \mid \bar{R}|$ is that of the eigenvectors of the small problem.

$(iv)'$ $X = |Y \mid \bar{Y}|\,R$ is calculated ($\bar{X}$ is not calculated). The modifications presented in steps $(i)'$–$(iv)'$ allow about a twofold decrease in the amount of computation and computer memory required.

4. TWO-DIMENSIONAL PROBLEMS. DISCRETIZATION AND SOLUTION

Let us consider the problems of eigen electromagnetic modes (waves) in longitudinally homogeneous and axially symmetric structures, reduced to two-dimensions. In doing this, we shall begin with simpler scalar problems, i.e., with the modes in longitudinal homogeneous systems, then come to axially symmetric modes in axially symmetric cavities, and finish with the vector problem for nonsymmetric modes in axially symmetric periodic structures.

4.1. System Homogeneous in z

The waves *TM* and *TE* in systems homogeneous along z are characterized by the components e_z and h_z, respectively. Let w denote either e_z or h_z; then for w we

have the problem

$$\nabla_\perp^2 w + \chi^2 w = 0, \tag{15}$$

with boundary conditions

$$w|_{C_1} = 0, \qquad w|_{C_2} = 0, \quad \text{or} \quad \left.\frac{\partial w}{\partial \nu}\right|_{C_2} = 0 \tag{16}$$

for the *TM* wave, and

$$\left.\frac{\partial w}{\partial \nu}\right|_{C_1} = 0, \quad \left.\frac{\partial w}{\partial \nu}\right|_{C_2} = 0, \quad \text{or} \quad w|_{C_2} = 0 \tag{17}$$

for the *TE* wave. Here $\nabla_\perp \equiv \left(\frac{\partial}{\partial x}, \frac{\partial}{\partial y}\right)$, C_1 is the metal contour in the plane (x, y), C_2 is the symmetry plane (if any), and χ is the transverse wave number. The remaining field components are reconstructed in the known way from the value of w.[19]

The discretization of problem Eqs. (15)–(17) is performed in a standard way by the finite-element method.[13] Let the waveguide cross section in the (x, y) plane be broken into finite elements with any enumeration of nodes, $i = 1, \ldots, N$, and any system of the basis functions $\{\psi_i(x, y)\}$. Multiplying Eq. (15) by ψ_i and integrating by parts, we obtain

$$\int (\nabla_\perp \psi_i \nabla_\perp w - \chi^2 \psi_i w)\, ds = \int \psi_i \frac{\partial w}{\partial \nu}\, dC. \tag{18}$$

Expanding w in the basis $\{\psi_i\}$, $w = \sum_j w^j \psi_j$, where w^j are the node values of w, and putting it into Eq. (18), we obtain

$$\sum_j \int (\nabla_\perp \psi_i \nabla_\perp \psi_j - \chi^2 \psi_i \psi_j)\, ds \cdot w^j = \int \psi_i \frac{\partial w}{\partial \nu}\, dC. \tag{19}$$

The right-hand side of Eq. (19) is equal to zero for all inner nodes and for those on the boundary that have the condition of the second kind, because in this case $\psi_i|_C = 0$ or $(\partial w/\partial \nu)|_C = 0$. For the nodes on the boundary with the condition of the first kind, Eq. (19) should not be written, since the node values are already known: $w^j = 0$. So, having taken into account the boundary conditions given by Eqs, (16) and (17), we obtain the generalized eigenvalue problem$(A_{ij} - \chi^2 B_{ij})w^j = 0$, with symmetric positive-definite matrices $A_{ij} \equiv \int \nabla_\perp \psi_i \nabla_\perp \psi_j\, ds$ and $B_{ij} \equiv \int \psi_i \psi_j\, ds$, whose solution has been described in section 3 in steps (i)–(iv). The problem given in Eqs. (15)–(17) is used to simulate *H*-wave structures. As an example, Fig. 1 presents the cross section of a four-vane *H*-cavity and the shape of the first three modes. A kink specially introduced into the upper vane is seen to affect the symmetry of the field between the electrodes. If it were not for this kink, it would have been sufficient to consider an eighth part of the cavity cross section.

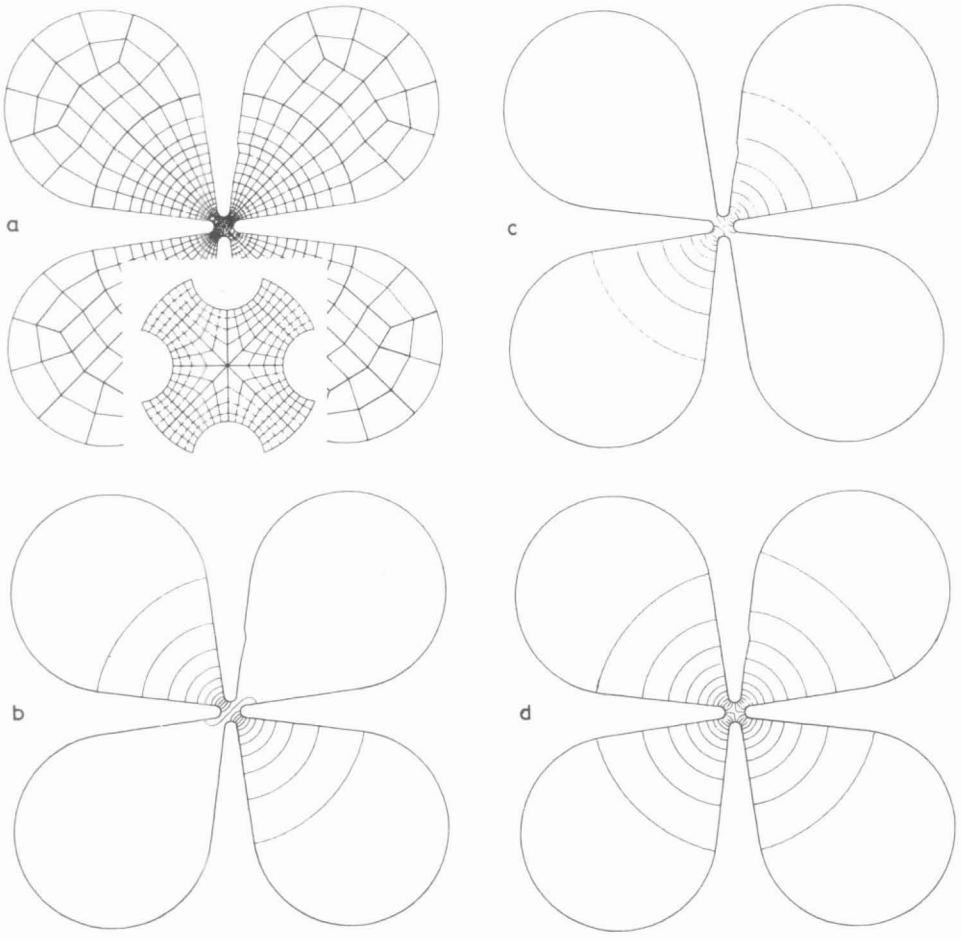

FIGURE 1 Four-vane H cavity: (a) finite element mesh, (b, c) dipole modes, (d) quadrupole mode.

4.2. Axially Symmetric Cavity

In axially symmetric cavities in the cylindric coordinate system (z, ρ, φ), there are two φ-independent types of waves: E waves with nonzero components (e_z, e_ρ, h_φ) and H waves with components (h_z, h_ρ, e_φ). For this case, the notations are

$$\mathbf{e}_\perp \equiv (e_z, e_\rho), \qquad \mathbf{h}_\perp \equiv (h_z, h_\rho), \qquad \nabla_\perp \equiv \left(\frac{\partial}{\partial z}, \frac{\partial}{\partial \rho}\right)$$

$$\mathbf{e}_\perp = \frac{1}{k\rho} \nabla_\perp \times \rho \mathbf{h}_\varphi, \qquad \mathbf{h}_\perp = \frac{1}{k\rho} \nabla_\perp \times \rho \mathbf{e}_\varphi.$$

Denoting $w = l_\varphi$ or $w = h_\varphi$, we obtain in the (z, ρ) plane

$$-\nabla_\perp \rho \nabla_\perp w + \frac{w}{\rho} - k^2 \rho w = 0. \tag{20}$$

Equation (20) is complemented by boundary conditions on the metal C_1, on the symmetry planes C_2 ($z = \text{const}$), and on the axis z: for E waves,

$$\rho \frac{\partial w}{\partial \nu} + \frac{\partial \rho}{\partial \nu} w\Big|_{C_1} = 0, \qquad \frac{\partial w}{\partial \nu}\Big|_{C_2} = 0, \quad \text{or} \quad w|_{C_2} = 0,\ w|_{\rho=0} = 0, \tag{21}$$

and for H waves,

$$w|_{C_1} = 0,\ w|_{C_2} = 0, \quad \text{or} \quad \frac{\partial w}{\partial \nu}\Big|_{C_2} = 0,\ w|_{\rho=0} = 0. \tag{22}$$

As in the case of section 4.1, we easily obtain an algebraic eigenvalue problem with the matrices

$$A_{ij} \equiv \int \left(\rho \nabla_\perp \psi_i \nabla_\perp \psi_j + \frac{1}{\rho} \psi_i \psi_j \right) ds + \int_{C_1} \frac{\partial \rho}{\partial \nu} \psi_i \psi_j \, dC \quad \text{and} \quad B_{ij} \equiv \int \rho \psi_i \psi_j \, ds.$$

Equations (20)–(21) describe, in particular, standing waves of the TM_0 type most commonly employed in linear accelerators. Figure 2 shows a cavity representing a section of a disk-and-washer (DAW) structure, connected with a coaxial bridge coupler. The structure of the field of the operating mode (the level lines of ρh_φ or the field lines of $\rho \mathbf{e}_\perp$) is shown in Fig. 2(b). Details of such cavities are described in Ref. 21.

4.3. *Infinite Chain of Cells*

Slight modifications allow us to go from the problem of Eqs. (20)–(22) to the calculation of any kind of axially symmetric wave (at any point of the dispersion

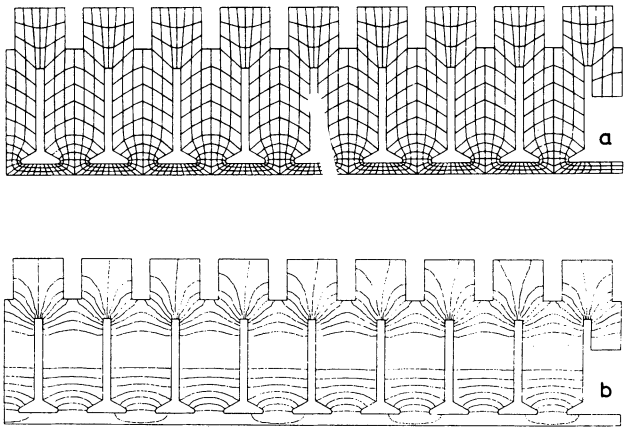

FIGURE 2 Mesh (a) and operating mode (b) in a section of a DAW structure with coaxial coupler.

characteristic) in an infinite chain of connected axially symmetric cells. Consider a periodic structure of period L. First, assume a cell $-L/2 \leq z \leq L/2$ to be symmetric about the plane $z = 0$. In this case, $w = u - iv$ is a complex function satisfying the equation

$$-\nabla_\perp \rho \nabla_\perp w + \frac{1}{\rho} w - k^2 \rho w = 0. \tag{23}$$

The boundary condition on the metal is

$$\rho \frac{\partial w}{\partial \nu} + \frac{\partial \rho}{\partial \nu} w|_{C_1} = 0 \quad \text{for } E \text{ waves}$$

and

$$w|_{C_1} = 0 \quad \text{for } H \text{ waves.} \tag{24}$$

The quasiperiodicity conditions in the form of Eqs. (11) and (12), in the planes $C_0(z = 0)$ and $C_+(z = L/2)$, have the form

$$\begin{aligned} \operatorname{Re} \frac{\partial w}{\partial z}\bigg|_{C_0} = 0, \qquad \operatorname{Im} w|_{C_0} = 0, \\ \operatorname{Re}\left(e^{i\theta/2} \frac{\partial w}{\partial z}\right)\bigg|_{C_+} = 0, \qquad \operatorname{Im}(e^{i\theta/2} w)|_{C_+} = 0, \end{aligned} \tag{25}$$

and also $w|_{\rho=0} = 0$.

Representing w in the form $w = \sum_j w^j \psi_j$ we routinely obtain

$$\sum_j C_{ij} w^j = \int \rho \psi_i \frac{\partial w}{\partial \nu} dc, \tag{26}$$

where

$$C_{ij} \equiv \int \left[\rho \nabla_\perp \psi_i \nabla_\perp \psi_j + \left(\frac{1}{\rho} - k^2 \rho\right) \psi_i \psi_j\right] ds.$$

Equation (26) and all the boundary conditions except those in the plane C_+ are real. Therefore, for all the nodes except those belonging to C_+, Eq. (26) simplifies into two equations for u and v. Should the node i be in the plane C_+, we shall have to multiply Eq. (26) by $e^{i\theta/2}$. Then, using the notation $w' = e^{i\theta/2} w = u' - iv'$, we obtain

$$\sum_j{}' C_{ij} w'^j + \sum_k{}'' C_{ik} e^{i\theta/2} w^k = \int \rho \psi_i \frac{\partial w'}{\partial \nu} dC.$$

Here the sum Σ' is taken over all nodes $j \in C_+$, and Σ'' is taken over the remaining inner nodes. Separating the real and imaginary parts and taking into account Eq. (25), we obtain

$$\sum_j{}' C_{ij} u'^j + \sum_k{}'' C_{ik} \cos \frac{\theta}{2} u^k + \sum_k{}'' C_{ik} \sin \frac{\theta}{2} v^k = 0, \qquad v'^i = 0. \tag{27}$$

Now we write Eq. (26) for some fixed inner node k belonging to the sum Σ'' in

Eq. (27):

$$\sum_i{}' C_{ki} e^{-i\theta/2} w'^i + \sum_j C_{kj} w^j = 0$$

or

$$\sum_i{}' C_{ki} \cos\frac{\theta}{2} u'^i + \sum_j{}'' C_{kj} u^j = 0,$$

$$\sum_i{}' C_{ki} \sin\frac{\theta}{2} u'^i + \sum_j{}'' C_{kj} v^j = 0. \tag{28}$$

As seen from Eqs. (27) and (28), for the variables u^i, v^i ($i \notin C_+$) and u'^i, v'^i ($i \in C_+$), we arrive again at a symmetric algebraic eigenvalue problem.

To illustrate this approach we shall present the results of the calculation of E waves in a periodic Alvarez structure, whose dimensions have been borrowed from Ref. 10. Figure 3 shows seven lower branches of the dispersion characteristics, and the circles are used to denote the calculated points. For $\theta = 0$ and $\theta = \pi$, the circles denote the modes symmetric about the plane $z = 0$, and the crosses

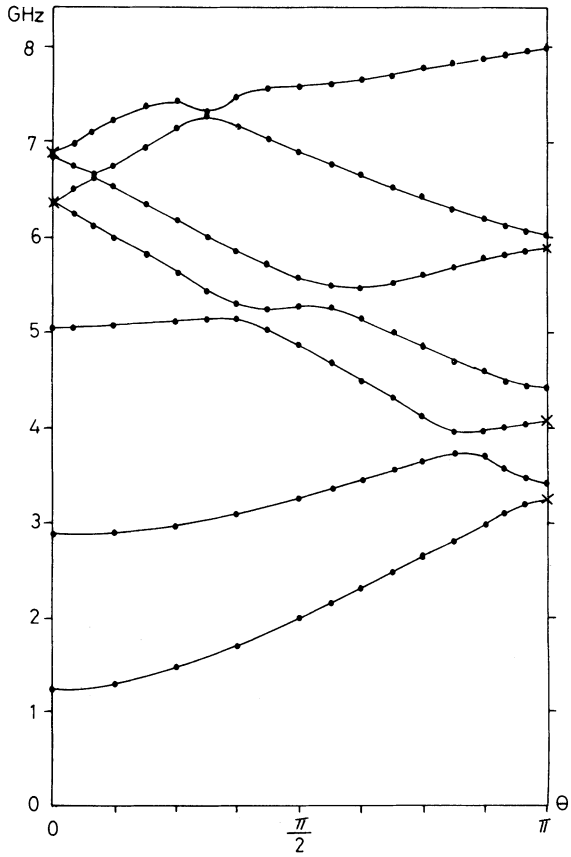

FIGURE 3 Branches of $\omega - \theta$ diagram of an Alvarez structure (see Ref. 10).

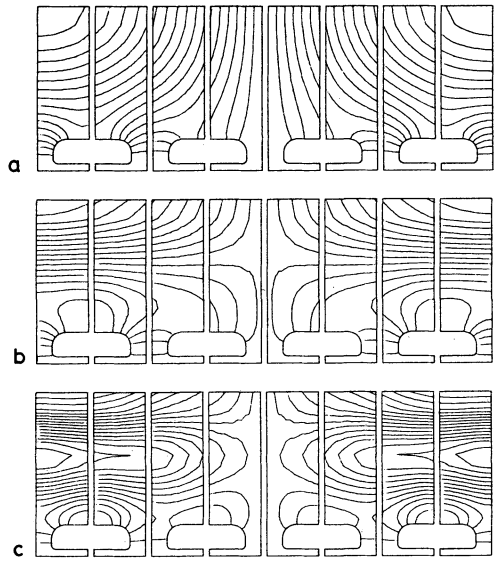

FIGURE 4 $\pi/4$ waves in the Alvarez structure, corresponding to the three lowest branches of Fig. 3.

denote antisymmetric ones. Figure 4 presents the field lines of $\rho\mathbf{e}$ corresponding to the points $\theta = \pi/4$ for the three lower branches. The fields in the cells have been reconstructed with the help of Eqs. (7) and (25) from the values calculated for the first half-cell.

For the endpoints of the dispersion curves, $\theta = 0$, and $\theta = \pi$, the problem given by Eqs. (23)–(25) is broken into two independent problems for u and v whose spectra do not coincide. Thus, for the endpoints, there is, generally speaking, an alternative, $u \not\equiv 0$, $v \equiv 0$ or $u \equiv 0$, $v \not\equiv 0$. Yet, there may exist a frequency which is the eigenvalue of either problem. This signifies coincidence of the two points of the dispersion branches; therefore, the structure is referred to as a compensated one.[9] A DAW structure[6] may serve as an example, because the frequency of its operating π mode coincides with that of the coupling π mode. A high stability of the operating field with respect to various types of perturbations[6,9] is a most important property of compensated structures.

4.4. Asymmetric Period

The next step is to generalize the problem from section 4.3 to the case of an asymmetric period. We consider a periodic structure with periodic cell $-L/2 \leqslant z \leqslant L/2$. The distinctive feature of this problem, as opposed to the previous one, is the fact that the local boundary conditions (Eq. (25)] in the planes C_0 and C_+ on a half-cell are replaced by nonlocal ones in the planes $C_-(z = -L/2)$ and $C_+(z = L/2)$ on a full cell:

$$w|_{C_+} = e^{-i\theta} w|_{C_-}, \qquad \left.\frac{\partial w}{\partial v}\right|_{C_+} = -e^{-i\theta} \left.\frac{\partial w}{\partial v}\right|_{C_-}. \tag{29}$$

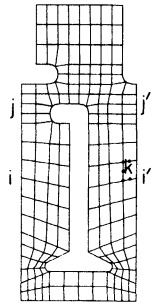

FIGURE 5 Structure cell without a symmetry plane.

Let a finite element mesh have the same layout of nodes in the planes C_- and C_+, so that each node j of the left boundary corresponds to the node j' of the right one (see Fig. 5). Let us write Eq. (26) for the nodes $i \in C_-$ and $i' \in C_+$:

$$\sum_l C_{il} w^l = \int_{C_-} \rho \psi_i \frac{\partial w}{\partial \nu} dC, \qquad \sum_k C_{i'k} w^k = \int_{C_+} \rho \psi_{i'} \frac{\partial w}{\partial \nu} dC.$$

Multiplying the second equation by $e^{i\theta}$ and adding the product to the first one, and also taking into account Eq. (29) (the equality $\psi_i|_{C_-} = \psi_{i'}|_{C_+}$ is apparent), we obtain the equation

$$(C_{ii} + C_{i'i'}) w^i + \sum_{l \neq i} C_{il} w^l + \sum_{k \neq i'} C_{i'k} e^{i\theta} w^k = 0. \tag{30}$$

The equation for w^k will be written in the form

$$\sum_{n \neq i'} C_{kn} w^n + C_{ki'} e^{-i\theta} w^i = 0. \tag{31}$$

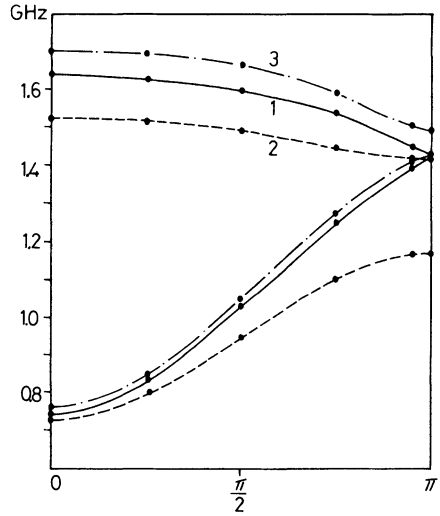

FIGURE 6 Branches of $\omega - \theta$ diagram for the structures in Fig. 7: symmetric cell (curve 1), cell with peripheral asymmetry (curve 2), and cell with asymmetric drift tube (curve 3).

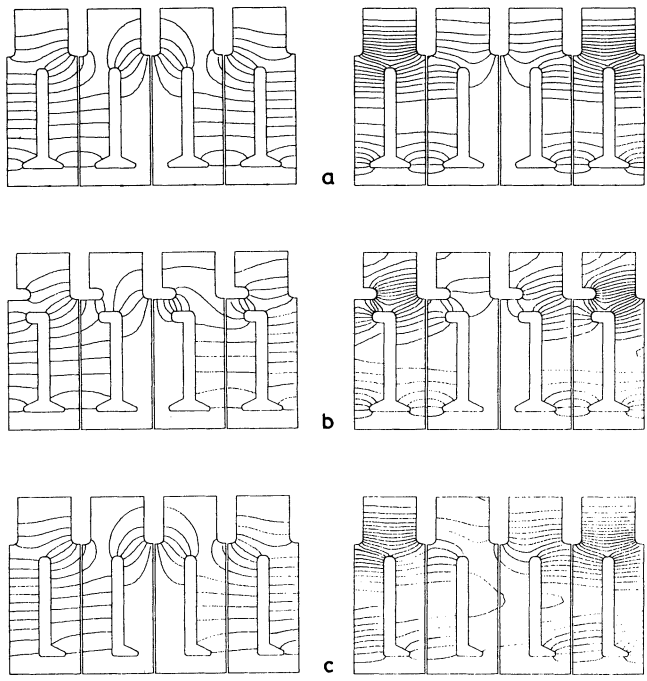

FIGURE 7 $\pi/4$ waves in various variants of a structure: (a) symmetric cell, (b) cell with peripheral asymmetry, and (c) cell with asymmetric drift tube.

Equations (30) and (31) suggest that w^i is coupled with w^k by the coefficient $C_{i'k}e^{i\theta}$ and w^k is coupled with w^i by $C_{ki'}e^{-i\theta}$. In this case, $(C_{i'k}e^{i\theta})^* = C_{ki'}e^{-i\theta}$. The symmetry of the remaining couplings is evident. Thus, we obtain an algebraic eigenvalue problem with Hermitian matrices, whose solution is given in section 3 in the form of steps (i)–(iv). The phase uncertainty of the wave in Eqs. (23), (24), and (29) is reflected by the multiplicity of the eigenvalues of the problem with extened matrices [Eq. (14)].

Figures 6 and 7 relate to three variants of DAW structures: a symmetric cell, a cell with peripheral asymmetry, a cell with an asymmetric drift tube. It should be noted that distortions have been made for illustrative purposes only. Each variant of the structure in Fig. 6 has two branches of the dispersion characteristic, and each one in Fig. 7 has field lines $\rho\mathbf{e}_\perp$ corresponding to the points $\theta = \pi/4$. In all the examples, the wave phases at one of the points of the left boundary were chosen to be equal to zero.

4.5. Azimuthally Varying Modes

The search for modes with azimuthal variation is a more complicated problem. According to our estimates, the solution presented below is more efficient than those offered by Refs. 1 and 22.

Suppose we have an axially symmetric cavity and w denotes either $\mathbf{e}$ or $\mathbf{h}$,

where $\mathbf{e} = (e_z, e_\rho, e_\varphi)$ and $\mathbf{h} = (h_z, h_\rho, h_\varphi)$ are the field amplitudes obtained after extraction of the harmonic dependence in φ (see, for instance, Ref. 22), i.e., depending on the coordinates (z, ρ) only. Then the wave equation [Eq. (4)] takes the form

$$\begin{aligned}
&-\nabla_\perp \rho \nabla_\perp w_z + \left(\frac{n^2}{\rho} - k^2\rho\right) w_z = 0, \\
&-\nabla_\perp \rho \nabla_\perp w_\rho + \left(\frac{n^2+1}{\rho} - k^2\rho\right) w_\rho + \frac{2n}{\rho} w_\varphi = 0, \\
&-\nabla_\perp \rho \nabla_\perp w_\varphi + \left(\frac{n^2+1}{\rho} - k^2\rho\right) w_\varphi + \frac{2n}{\rho} w_\rho = 0.
\end{aligned} \tag{32}$$

We shall need these equations in a more general form or, putting it more precisely, in the projections on the axis (x_1, x_2, φ) turned in the plane (z, ρ) to an angle α with respect to the axis (z, ρ, φ), so that $\mathbf{w}$ has the components (w_1, w_2, w_φ). It is not difficult to obtain the following system:

$$\begin{aligned}
&-\nabla_\perp \rho \nabla_\perp w_1 + \left[\left(\frac{\partial \rho}{\partial x_1}\right)^2 \frac{1}{\rho} + \frac{n^2}{\rho} - k^2\rho\right] w_1 + \frac{\partial \rho}{\partial x_1}\frac{\partial \rho}{\partial x_2}\frac{1}{\rho} w_2 + \frac{\partial \rho}{\partial x_1}\frac{2n}{\rho} w_\varphi = 0, \\
&-\nabla_\perp \rho \nabla_\perp w_2 + \left[\left(\frac{\partial \rho}{\partial x_2}\right)^2 \frac{1}{\rho} + \frac{n^2}{\rho} - k^2\rho\right] w_2 + \frac{\partial \rho}{\partial x_2}\frac{\partial \rho}{\partial x_1}\frac{1}{\rho} w_1 + \frac{\partial \rho}{\partial x_2}\frac{2n}{\rho} w_\varphi = 0, \\
&-\nabla_\perp \rho \nabla_\perp w_\varphi + \left[\frac{n^2+1}{\rho} - k^2\rho\right] w_\varphi + \frac{\partial \rho}{\partial x_1}\frac{2n}{\rho} w_1 + \frac{\partial \rho}{\partial x_2}\frac{2n}{\rho} w_2 = 0.
\end{aligned} \tag{33}$$

Note that $\partial\rho/\partial x_1 = \sin\alpha$ and $\partial\rho/\partial x_2 = \cos\alpha$. Let us write the boundary conditions given by Eqs. (5) and (6) for Eqs. (32). Let (ν, τ) be a local coordinate system connected with boundary contours in the plane (z, ρ) in a natural way. Then the conditions of Eq. (5) take the form

$$w_\varphi = 0, \qquad w_\tau = 0, \qquad \rho \frac{\partial w_\nu}{\partial \nu} + w_\nu \left(\frac{\partial \rho}{\partial \nu} \pm \frac{\rho}{r}\right) = 0, \tag{34}$$

where r is the local curvature radius of the contour, with the "+" indicating a boundary convex to the normal and the "−" indicating the opposite. The conditions of Eq. (6) take the form

$$\rho \frac{\partial w_\varphi}{\partial \nu} + \frac{\partial \rho}{\partial \nu} w_\varphi = 0, \; w_\nu = 0, \; \frac{\partial w_\tau}{\partial \nu} \pm \frac{w_\tau}{r} = 0. \tag{35}$$

It is necessary to recall that Eqs. (34) and (35) refer to the boundary conditions on a metal providing $\mathbf{w} = \mathbf{e}$ and $\mathbf{w} = \mathbf{h}$, respectively. We choose either Eq. (34) or (35) on the symmetry planes $z = \text{const}$, depending on the symmetry of the modes sought. In this case, the expressions are simply

$$w_\varphi = 0, \; w_\rho = 0, \; \frac{\partial w_z}{\partial z} = 0, \tag{34a}$$

$$\frac{\partial w_\varphi}{\partial z} = 0, \; \frac{\partial w_\rho}{\partial z} = 0, \; w_z = 0. \tag{35a}$$

On the z axis,

$$w_z = \frac{\partial w_\rho}{\partial \rho} = \frac{\partial w_\varphi}{\partial \rho} = 0, \quad n = 1,$$
$$w_z = w_\rho = w_\varphi = 0, n > 1. \tag{36}$$

To obtain the discrete approximation, we shall, as usual, put $\mathbf{w}$ in the form $\mathbf{w} = \sum_j \mathbf{w}^j \psi_j$. The node values $\mathbf{w}^j$ will be projected in all inner nodes of the mesh onto the axis (z, ρ, φ), and those in the nodes on the metal boundary will be projected onto the directions (ν, τ, φ). Multiplying Eqs. (32) by ψ_i and integrating, we have equations for w_z^i, w_ρ^i, and w_φ^i in each inner node:

$$\sum_j \begin{vmatrix} a_{ij} & 0 & 0 \\ 0 & a_{ij} + b_{ij} & 2nb_{ij} \\ 0 & 2nb_{ij} & a_{ij} + b_{ij} \end{vmatrix} \begin{vmatrix} w_z^j \\ w_\rho^j \\ w_\varphi^j \end{vmatrix} \equiv \sum_j M_{ij} \begin{vmatrix} w_z^j \\ w_\rho^j \\ w_\varphi^j \end{vmatrix}, \tag{37}$$

where

$$a_{ij} = \int \left[\rho \nabla_\perp \psi_i \nabla_\perp \psi_j + \left(\frac{n^2}{\rho} - k^2 \rho \right) \psi_i \psi_j \right] ds, \qquad b_{ij} \equiv \int \frac{1}{\rho} \psi_i \psi_j. \tag{38}$$

For the boundary node i from Eqs. (33), there follow equations for $(w_1^i, w_2^i, w_\varphi^i)$:

$$\sum_j \begin{vmatrix} a_{ij} + b_{ij} \sin^2 \alpha & b_{ij} \sin \alpha \cos \alpha & b_{ij} 2n \sin \alpha \\ b_{ij} \sin \alpha \cos \alpha & a_{ij} + b_{ij} \cos^2 \alpha & b_{ij} 2n \cos \alpha \\ b_{ij} 2n \sin \alpha & b_{ij} 2n \cos \alpha & a_{ij} + b_{ij} \end{vmatrix} \begin{vmatrix} w_1^j \\ w_2^j \\ w_\varphi^j \end{vmatrix} \equiv \sum_j M'_{ij} \begin{vmatrix} w_1^j \\ w_2^j \\ w_\varphi^j \end{vmatrix} = \begin{vmatrix} I_1^i \\ I_2^i \\ I_3^i \end{vmatrix}, \tag{39}$$

where

$$I_1^i = \int \rho \psi_i \frac{\partial w_1}{\partial \nu} dC, \qquad I_2^i = \int \rho \psi_i \frac{\partial w_2}{\partial \nu} dC, \qquad I_3^i = \int \rho \psi_i \frac{\partial w_\varphi}{\partial \nu} dC. \tag{40}$$

All $\mathbf{w}^j$ in Eq. (39) are implied to be projected onto the axis (x_1, x_2, φ). When integrating by the element boundary, $\frac{\partial w_1}{\partial \nu}$ and $\frac{\partial w_2}{\partial \nu}$ of Eqs. (40) can be replaced by $\frac{\partial w_\nu}{\partial \nu}$ and $\frac{\partial w_\tau}{\partial \nu}$ to an accuracy of $O\left(\frac{\delta C}{r}\right)$, and then the conditions of Eqs. (34) and (35) can be applied; δC is the linear dimension of the element. And, finally, to come to the end of the problem, the relation between the projections $\mathbf{w}^i$ in the inner nodes with those $\mathbf{w}^j$ in the nodes on the boundary in Eq. (37) and the inverse relation in Eq. (39) remain to be established. Let (i, j) be a fixed pair of indices belonging simultaneously to the sums in Eqs. (37) and (39) and let it be an inner node and j a boundary one. Taking into account that $\mathbf{w}^i$ and $\mathbf{w}^j$ are projected in different coordinate systems in Eqs. (37) and (39), we shall make the appropriate replacements:

$$\begin{vmatrix} w_z^j \\ w_\rho^j \\ w_\varphi^j \end{vmatrix} = \begin{vmatrix} \cos \alpha & -\sin \alpha & 0 \\ \sin \alpha & \cos \alpha & 0 \\ 0 & 0 & 1 \end{vmatrix} \begin{vmatrix} w_1^j \\ w_2^j \\ w_\varphi^j \end{vmatrix} \equiv P \begin{vmatrix} w_1^j \\ w_2^j \\ w_\varphi^j \end{vmatrix}, \quad \begin{vmatrix} w_1^i \\ w_2^i \\ w_\varphi^i \end{vmatrix} = P^T \begin{vmatrix} w_z^i \\ w_\rho^i \\ w_\varphi^i \end{vmatrix}. \tag{41}$$

Then matrix elements coupling the components $\mathbf{w}^i$ and $\mathbf{w}^j$ in Eq. (37) and $\mathbf{w}^j$ and $\mathbf{w}^i$ in Eq. (39) are equal to $M_{ij}P$ and $M'_{ji}P^T$. Direct multiplication allows us to verify easily that

$$(M_{ij}P)^T = M'_{ji}P^T,$$

which means symmetry of the complete matrix.

Before coming to examples, let us make the following remarks. First, by repeating the reasoning of section 4.3. and 4.4, the problem of Eqs. (32)–(36) is easily complemented by the periodicity condition of Eqs. (6) for an arbitrary period and by Eqs. (11) and (12) for a symmetric one, and thus a waveguide problem is also formulated. Second, in the neighborhood of the angle convexity, the field has a singularity (so-called condition on the edge).[4,5] For the discrete approximations to be correct in the neighborhood of such an angle, it should be smoothed and then the mesh should be made finer so that the term $O\left(\frac{\delta C}{r}\right)$ could be neglected. Third, in order to reject potential solutions, $\gamma = \int |\nabla \times \mathbf{w}|^2 \, ds/k^2 \int |\mathbf{w}|^2 \, ds$ is calculated for each vector obtained [see Eqs. (9)]. As proved practically, on a fairly good mesh, the values of γ are within the range

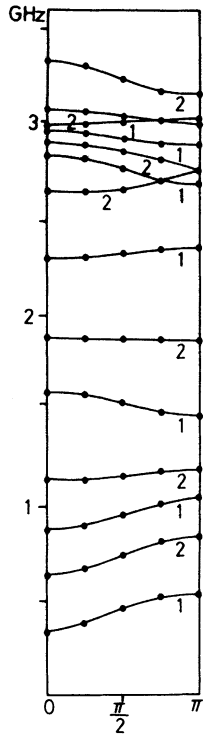

FIGURE 8 Branches of $\omega - \theta$ diagram for transverse waves in the DAW structure for $n = 1$ (curves 1) and $n = 2$ (curves 2).

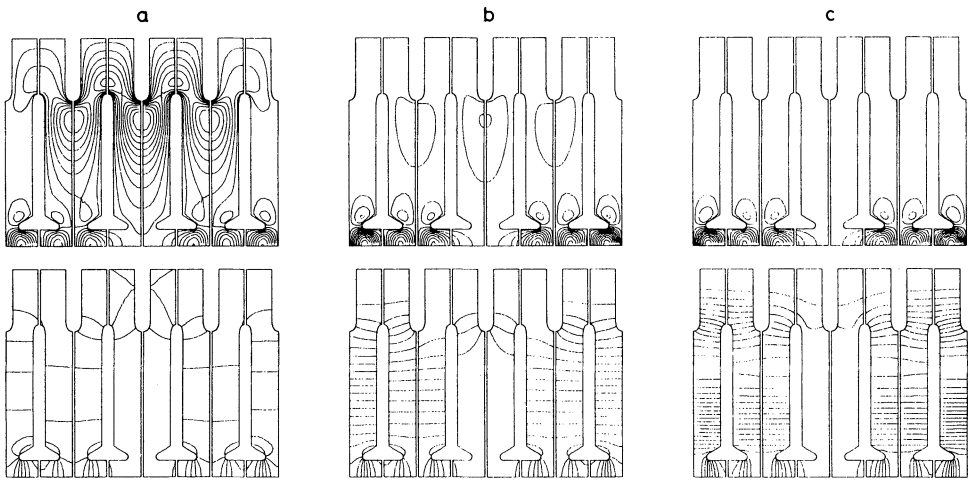

FIGURE 9 Isolines of l_φ and h_φ for $\pi/4$ waves with $n = 1$ for the three lowest branches in Fig. 8.

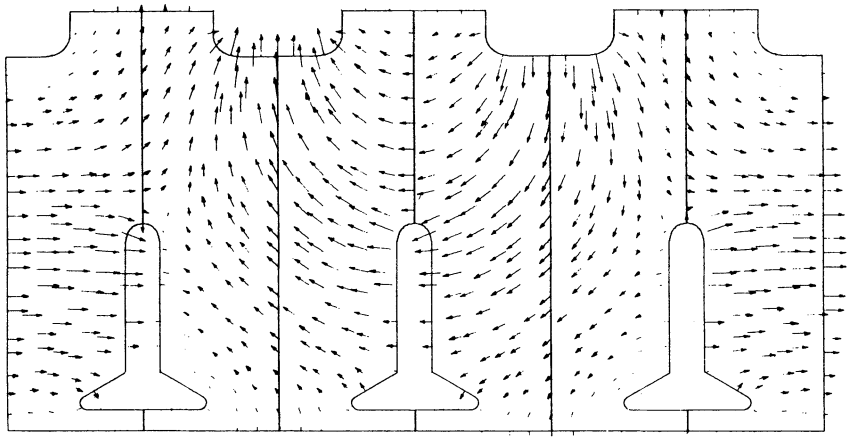

FIGURE 10 E field of $\frac{2}{3}\pi$ wave of EH_{11} type in the DAW structure.

0.999 to 1.0 for vortex solutions and 0 to 10^{-3} for potential ones. This means that we have a quality criterion. These and other algoritmic questions of code realization are presented in detail in Refs 23–28.

Figure 8 presents the computed dispersion characteristics of waves with one and two variations over the azimuth in a DAW structure, whose dimensions are the same as in Ref. 29. Figure 9 shows the isolines h_φ and e_φ for the points $\theta = \pi/4$ of three lower branches for the modes with one variation. The fields in the cells have been reconstructed from the values of those in the first half-cell. The data are presented in more detail in Ref. 28. Figure 10 shows the vector field $\mathbf{e}_\perp$ of the $\theta = \frac{2}{3}\pi$ wave of type EH_{11} for one of the structure variants.

5. BRIEF DETAIL OF THE PACKAGE

The above technique has been incorporated in the program package PRUD-W, consisting of the modules GENER, PRUDW, SQUANT, and PPLOT.

GENER is the mesh generator of 8-node isoparametric elements. Examples has been presented above.

PRUDW is the basic program of the package, designed to search for eigenfrequencies and eigenvectors.

SQUANT computes secondary quantities necessary for applications. These are as follows: the remaining field components, the field energy in the cavity volume (or per unit waveguide length), magnetic and electric energy in the specified subregions, the density of power losses in the metal and the total losses, Q quality, the shunt impedance, and the transit time factors. All dimensional quantities are, if required, normalized to values of the electromagnetic energy and the voltage on axis. As far as the problem of section 4.1 is concerned, the voltage along the specified path is taken.

PPLOT outputs meshes, vector fields, the isolines of field components, etc., on the plotter.

To check whether the program and its blocks are running correctly and to estimate the accuracy, time, and feasibility of computing modes with multiple eigenvalues, we have treated the problems having an analytical solution, i.e., modes in cylindrical and spherical cavities. The results are presented in detail in Refs. 23–28. It should be stressed that from the viewpoint of accuracy and time consumption the code PRUD-W is an order of magnitude better than those discussed in Refs. 1 and 11. Besides, it presents fundamentally new possibilities for obtaining the dispersion characteristics of periodic structures. This is connected with unconditional and fast convergence of the subspace iteration method (independent of the initial approximation)[14,23] and the possibility of obtaining simultaneously a few (up to 10–15) eigenvectors. Setting the phase shift and the number of vectors to be iterated, one can obtain points all at once on a few branches of the dispersion characteristic.

ACKNOWLEDGMENTS

The authors are sincerely indebted to A. G. Abramov, T. D. Ryabova, and S. Yu. Yershov for their participation in this work at its various stages, and also to V. A. Teplyakov and V. D. Zhilchenkov for helpful discussions and kind support.

REFERENCES

1. T. Weiland, *Nucl. Instrum. Methods Phys. Res.* **216,** 329 (1983).
2. T. Weiland, DESY Preprint 84-006 (1984).
3. E. Keil, CERN Preprint 84-01 (1984).

4. R. Mittra and S. W. Lee, *Analytical Techniques in the Theory of Guided Waves* (Macmillan, New York, 1971).
5. A. S. Ilyinsky and G. Ya. Slepyan, *Oscillations and Waves in the Electrodynamic Systems with Losses* (MGU, Moscow, 1983).
6. V. G. Andreev, *JETP Lett.* **41,** 788 (1971).
7. E. Keil, *Nucl. Instrum. Methods* **100,** 419 (1972).
8. B. Zotter and K. Bane, PEP Note 308 (1979).
9. G. Dôme and P. Lapostolle, in *Proc.* 1968 *Proton Linear Accelerator Conference,* BNL 50120 (1968).
10. M. Bell and G. Dôme, CERN Preprint 73-1 (1973).
11. K. Halbach and R. F. Holsinger, *Particle Accelerators* **7,** 213 (1976).
12. G. A. Loew *et al.*, SLAC PUB-2295 (1979).
13. G. Strang and G. J. Fix, *An Analysis of the Finite Element Method* (Prentice-Hall, Englewood Cliffs, NJ, 1973).
14. H. Rutishauser, *Numer. Math.* **13,** 4 (1969).
15. J. H. Wilkinson, *The Algebraic Eigenvalue Problem* (Clarendon, Oxford, 1965).
16. J. H. Wilkinson and C. Reinsch, *Handbook for Automatic Computation Linear Algebra* (Springer-Verlag, Berlin).
17. B. N. Parlett, *The Symmetric Eigenvalue Problem* (Prentice-Hall, Englewood Cliffs, NJ, 1980).
18. V. V. Nickolsky, *The Variational Methods for the Internal Electrodynamic Problems* (Nauka, Moscow, 1967).
19. V. V. Nickolsky, *The Electrodynamics and the Wave Propagation* (Nauka, Moscow, 1978).
20. A. B. Barsukov *et al.* Serpukhov IHEP 82-178 Preprint (1982).
21. A. G. Daikovsky *et al.*, Serpukhov IHEP 83-123 Preprint (1983).
22. A. G. Daikovsky *et al.*, *Particle Accelerators* **12,** 59 (1982).
23. A. G. Abramov *et al.*, Serpukhov IHEP 83-03 Preprint (1983).
24. Yu. I. Portugalov, Serpukhov IHEP 83-02 Preprint (1983).
25. A. G. Abramov *et al.* Serpukhov IHEP 83-179 Preprint (1983).
26. A. G. Abramov *et al.*, Serpukhov IHEP 83–178 Preprint (1983).
27. A. G. Daikovsky *et al.*, Serpukhov IHEP 84-40 Preprint (1984).
28. A. G. Daikovsky *et al.*, Serpukhov IHEP 84-103 Preprint (1984).
29. V. G. Andreev *et al.*, *Nucl. Instrum. Methods Phys. Res.* **204,** 285 (1983).